JCTC Journal of Chemical Theory and Computation

Combined Electrostatically Embedded Multiconfiguration Molecular Mechanics and Molecular Mechanical Method: Application to Molecular Dynamics Simulation of a Chemical Reaction in Aqueous Solution with Hybrid Density Functional Theory

Masahiro Higashi and Donald G. Truhlar*

Department of Chemistry and Supercomputing Institute, 207 Pleasant Street SE, University of Minnesota, Minneapolis, Minnesota 55455-0431

Received March 07, 2008

Abstract: We here combine the electrostatically embedded multiconfiguration molecular mechanics (EE−MCMM) method for generating global potential energy surfaces in the presence of an electrostatic potential with molecular mechanics (MM). The resulting EE−MCMM/MM method is illustrated by applying it to carry out a molecular dynamics simulation for the symmetric bimolecular reaction $Cl^- + CH_3Cl' \rightarrow ClCH_3 + Cl'^-$ in aqueous solution with hybrid density functional theory as the quantum mechanical level. The potential of mean force is calculated, and the free energy barrier is found to be 25.3 kcal/mol, which is in good agreement with previous work. The advantage of the combined EE−MCMM and MM method is that the number of quantum mechanical calculations required for the active subsystem is very small compared to straight direct dynamics.

1. Introduction

Combined quantum mechanical and molecular mechanical (QM/MM) methods have provided powerful means for studying chemical reactions in solution, enzymes, and solids.[1–35] In this approach, an active zone, which can be a solute molecule or the reaction center involved in the formation and breaking of chemical bonds, is described quantum mechanically, while the surroundings (e.g., the solvent or protein environment) are treated by using a molecular mechanics (MM) force field. When the system contains a large number of atoms, a statistical sampling method such as molecular dynamics (MD) or Monte Carlo simulation is required. However, the high computational cost of high-level *ab initio* or density functional QM calculations prevents carrying out QM/MM MD simulations for most catalytic and other condensed-phase reactions with reliable accuracy and adequate sampling.

Recently, we proposed a new method called electrostatically embedded multiconfiguration molecular mechanics (EE−MCMM) for generating global or semiglobal potential energy surfaces (PESs) in the presence of an electrostatic potential.[36] The new method is based on the QM/MM methodology, and it extends the domain of applicability of the multiconfiguration molecular mechanics (MCMM) method,[37] which has been successful[37–44] in describing semiglobal potential energy surfaces of gas-phase reactions and calculating their reaction rates with multidimensional tunneling contributions. Because the method is efficient, we can use DF/MM, that is, QM/MM with the QM level being density functional theory. We applied the new method to the symmetric bimolecular reaction $Cl^- + CH_3Cl' \rightarrow ClCH_3 + Cl'^-$ in aqueous solution; this reaction is a standard test case that has been investigated with various theoretical methods.[2,45–68] We compared the EE−MCMM potential energy with the directly evaluated electrostatically embedded QM energy, for which we used geometries and electrostatic potentials calculated by the reference interaction site model−self-consistent field method,[69–71] and we found that the potential energy in aqueous solution calculated by the new method is very close to that calculated directly without any fitting, although the EE−MCMM calculations required only a limited amount of electronic structure information for the gas-phase reaction in a field and no liquid-phase electronic structure calculations.

In the present paper, we develop the EE−MCMM method further. We apply the EE−MCMM method to full QM/MM MD simulations by replacing the electrostatically embedded QM energy with the EE−MCMM energy; we label the resulting potential energy surface as EE−MCMM/MM. EE−MCMM can reproduce global PESs calculated by high-level QM calculations in the presence of an electrostatic potential with a computational cost that is much lower than the cost of direct dynamics. Therefore, EE−MCMM/MM MD simulations can be carried out with high-level QM calculations, and adequate sampling is possible even when one uses high-level QM methods for a process requiring rare-event sampling (such as umbrella sampling).

The organization of the article is as follows. In the next section, we describe the theoretical methods employed here and derive the equations needed for the EE−MCMM/MM MD simulations. We then apply the EE−MCMM/MM method to the $Cl^- + CH_3Cl' \rightarrow ClCH_3 + Cl'^-$ reaction in aqueous solution.

* Corresponding author e-mail: truhlar@umn.edu.

10.1021/ct8000816 CCC: $40.75
Published on Web 05/29/2008

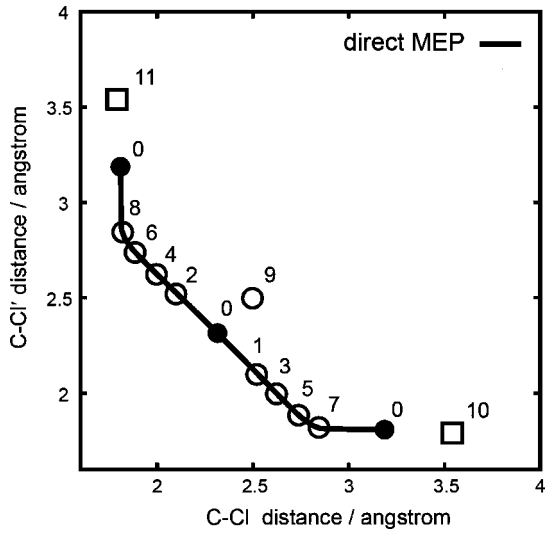

Figure 1. Gas-phase calculations: two-dimensional representation of the direct MEP and the location of Shepard points for the EE−MCMM calculation. Filled circles are stationary points; open circles are nonstationary Shepard points used in the previous and present studies; open squares are nonstationary Shepard points used in the present study.

In section 3, we present the computational details, and in section 4 we present and discuss the results of the calculations; the potential of mean force (PMF) is calculated, and the free energy of activation is compared with previous work. We also calculate the interaction energy and the radial distribution function between the QM and MM regions at the reactant and transition state. The conclusions are summarized in section 5.

2. Theoretical Method

Our goal is to calculate the Born−Oppenheimer potential energy surface V of a large system divided into a QM zone with N^{QM} atoms and a MM zone with N^{MM} atoms. The first component of V is the electrostatically embedded QM energy V^{EEQM}. We adopt a site−site representation of the QM/MM electrostatic interaction.[67,69,72–75] Then, we have

$$V^{\mathrm{EEQM}}(\mathbf{R},\mathbf{\Phi}) = \langle \Psi | \hat{H}_0 + \hat{\mathbf{Q}}^{\mathsf{T}}\mathbf{\Phi} | \Psi \rangle \tag{1}$$

where $\mathbf{R}$ stands for the collection of the coordinates $\mathbf{R}_a$ ($a = 1, 2,..., N^{\mathrm{QM}}$) of atoms in the QM region, Ψ is the electronic wave function, $\hat{H}_0$ is the electronic Hamiltonian (including nuclear repulsion) of the QM region, $\hat{\mathbf{Q}}$ is the population operator vector of order N^{QM} whose components $\hat{Q}_a$ are the population operators that generate the partial charges Q_a on QM atomic sites a:

$$Q_a = \langle \Psi | \hat{Q}_a | \Psi \rangle \tag{2}$$

and $\mathbf{\Phi}$ is the electrostatic potential distribution, which is a vector of order N^{QM}, each of whose components Φ_a is the electrostatic potential at atom a from the MM region,

$$\Phi_a(\mathbf{R},\mathbf{R}^{\mathrm{MM}}) = \sum_{A=1}^{N^{\mathrm{MM}}} \frac{Q_A^{\mathrm{MM}}}{|\mathbf{R}_a - \mathbf{R}_A^{\mathrm{MM}}|} \tag{3}$$

where $\mathbf{R}^{\mathrm{MM}}$ is the collection of the coordinates $\mathbf{R}_A^{\mathrm{MM}}$ of atom A in the MM region, and Q_A^{MM} is the effective charge of MM atom A. Note that the first derivative of V^{EEQM} with respect to Φ_a is given by[73]

$$\frac{\partial V^{\mathrm{EEQM}}}{\partial \Phi_a} = \langle \Psi | \hat{Q}_a | \Psi \rangle = Q_a \tag{4}$$

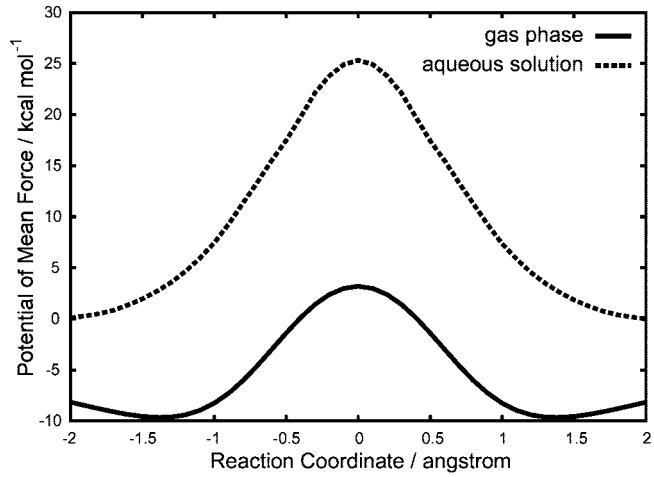

Figure 2. Potential energy profile of the $Cl^- + CH_3Cl' \rightarrow ClCH_3 + Cl'^-$ reaction in the gas phase (solid line) and potential of mean force of the reaction in the aqueous solution (dashed line). The gas-phase curve is relative to its value at $z = -\infty$, and the aqueous curve is relative to the value at reactants, at $z = -2.0$ Å.

Since details of the EE−MCMM method are presented elsewhere,[36] we describe the method only briefly in this Letter. The potential energy in EE−MCMM is the lowest eigenvalue of a 2 × 2 diabatic Hamiltonian matrix,

$$\mathbf{U}^{\mathrm{EE-MCMM}}(\mathbf{q},\mathbf{\Phi}) = \begin{pmatrix} U_{11}(\mathbf{q},\mathbf{\Phi}) & U_{12}(\mathbf{q},\mathbf{\Phi}) \\ U_{12}(\mathbf{q},\mathbf{\Phi}) & U_{22}(\mathbf{q},\mathbf{\Phi}) \end{pmatrix} \tag{5}$$

where $U_{11}(\mathbf{q},\mathbf{\Phi})$ and $U_{22}(\mathbf{q},\mathbf{\Phi})$ are analytic functions that describe V^{EEQM} in the regions of reactants and products, $U_{12}(\mathbf{q},\mathbf{\Phi})$ is explained in the next paragraph, and we use nonredundant or redundant internal coordinates[76] $\mathbf{q}$ to represent the nuclear coordinates of the QM subsystem. The lowest eigenvalue of eq 5 is given by

$$V^{\mathrm{EE-MCMM}}(\mathbf{q},\mathbf{\Phi}) = \frac{1}{2}\{[U_{11}(\mathbf{q},\mathbf{\Phi}) + U_{22}(\mathbf{q},\mathbf{\Phi})] - [(U_{11}(\mathbf{q},\mathbf{\Phi}) - U_{22}(\mathbf{q},\mathbf{\Phi}))^2 - 4U_{12}(\mathbf{q},\mathbf{\Phi})^2]^{\frac{1}{2}}\} \tag{6}$$

We evaluate $V^{\mathrm{EE-MCMM}}$ and its derivatives in terms of the internal coordinates $\mathbf{q}$;[37,77] then, we transform the derivatives to the Cartesian coordinate system $\mathbf{R}$: $\mathbf{V}^{\mathrm{EE-MCMM}}(\mathbf{q},\mathbf{\Phi}) \rightarrow \mathbf{V}^{\mathrm{EE-MCMM}}(\mathbf{R},\mathbf{\Phi})$.

The evaluation of $U_{12}(\mathbf{q},\mathbf{\Phi})$ is the key feature of the EE−MCMM algorithm. It is based on a set of interpolation nodes called Shepard points $(\mathbf{R}^{(k)},\mathbf{\Phi}^{(k)})$, where $k = 1, 2,..., N$. We evaluate $[U_{12}(\mathbf{q},\mathbf{\Phi};k)]^2$ by a second-order Taylor expansion around each Shepard point $(\mathbf{R}^{(k)},\mathbf{\Phi}^{(k)})$, where the Taylor series coefficients are determined such that $V^{\mathrm{EE-MCMM}}$ reproduces V^{EEQM} and its first and second derivatives with respect to $\mathbf{q}$ and $\mathbf{\Phi}$ at Shepard point $(\mathbf{R}^{(k)},\mathbf{\Phi}^{(k)})$. Then, we construct $U_{12}(\mathbf{q},\mathbf{\Phi})$ at any arbitrary geometry by Shepard interpolation[78,79] of these expressions.

The total potential energy V is obtained in the EE−MCMM/MM method by replacing the electrostatically embedded QM energy V^{EEQM} in the conventional QM/MM method with the EE−MCMM potential energy $V^{EE-MCMM}$; this yields

$$V(\mathbf{R}, \mathbf{R}^{MM}) = V^{EE-MCMM}(\mathbf{R}, \mathbf{\Phi}(\mathbf{R}, \mathbf{R}^{MM})) + V_{vdW}^{QM/MM}(\mathbf{R}, \mathbf{R}^{MM}) + V_{val}^{QM/MM}(\mathbf{R}, \mathbf{R}^{MM}) + V^{MM}(\mathbf{R}^{MM}) \quad (7)$$

where $V_{vdW}^{QM/MM}$ and $V_{val}^{QM/MM}$ are respectively the van der Waals and valence interaction energies between the QM and MM regions, and V^{MM} is the MM potential energy. MD simulations require the first derivatives of V with respect to $\mathbf{R}$ and $\mathbf{R}^{MM}$. These derivatives are given by

$$\frac{\partial V}{\partial \mathbf{R}_a} = \frac{\partial V^{EE-MCMM}}{\partial \mathbf{R}_a} + \frac{\partial V^{EE-MCMM}}{\partial \Phi_a}\frac{\partial \Phi_a}{\partial \mathbf{R}_a} + \frac{\partial V_{vdW}^{QM/MM}}{\partial \mathbf{R}_a} + \frac{\partial V_{val}^{QM/MM}}{\partial \mathbf{R}_a} \quad (8)$$

and

$$\frac{\partial V}{\partial \mathbf{R}_A^{MM}} = \sum_{a=1}^{N^{QM}} \frac{\partial V^{EE-MCMM}}{\partial \Phi_a}\frac{\partial \Phi_a}{\partial \mathbf{R}_A^{MM}} + \frac{\partial V_{vdW}^{QM/MM}}{\partial \mathbf{R}_A^{MM}} + \frac{\partial V_{val}^{QM/MM}}{\partial \mathbf{R}_A^{MM}} + \frac{\partial V^{MM}}{\partial \mathbf{R}_A^{MM}} \quad (9)$$

The terms involving V_{vdW}^{MM}, $V_{val}^{QM/MM}$, and V^{MM} are the same as in any other QM/MM method and need not be discussed. The derivatives of Φ_a are obtained analytically from eq 3. The first term of eq 8 is obtained analytically.[37,77] $\partial V^{EE-MCMM}/\partial \Phi_a$ is obtained by differentiating $V^{EE-MCMM}$ of eq 6 with respect to Φ_a as in eq 4 and equals the partial charge $Q_a^{EE-MCMM}$. Therefore, we can regard the electrostatic interaction between the QM and MM regions as

$$V_{ele}^{QM/MM} = \sum_{a}^{N^{QM}} Q_a^{EE-MCMM}\Phi_a \quad (10)$$

where

$$Q_a^{EE-MCMM} \equiv \frac{\partial V^{EE-MCMM}}{\partial \Phi_a} \quad (11)$$

3. Computational Details

We applied the EE−MCMM/MM method to the reaction $Cl^- + CH_3Cl' \rightarrow ClCH_3 + Cl'^-$ in aqueous solution. We took the difference between the two C−Cl distances as the reaction coordinate:

$$z = R_{CCl'} - R_{CCl} \quad (12)$$

Since the computational details of the EE−MCMM calculation in the present study are almost the same as those in the previous study,[36] we here describe them only briefly. We used the MPW1K density functional[80] for the electronic structure calculations on the QM subsystem. The basis set is 6-31G(d,p) for C and H atoms and 6-31+G(d,p) for Cl. We choose the population operator $\hat{Q}_a$ according to Charge Model 4 (CM4).[81] All of the electronic structure calculations were performed by a modified GAMESSPLUS[82] computer code based on the GAMESS quantum chemistry package.[83] In the EE−MCMM calculations, we used a modified[36] MM3 force field[84–86] for the diagonal elements. All of the EE−MCMM calculations were carried out by a new version of the MC-TINKER program.[77]

Table 1. Contributions to the QM/MM Electrostatic Interaction Energy From Individual Solute Atoms (in kcal/mol). Values in Parentheses are Standard Deviations.

	reactant	transition state
$\langle Q_C^{EE-MCMM}\Phi_C\rangle$	−14.3 (3.8)	0.8 (2.1)
$\langle Q_C^{EE-MCMM}\Phi_H\rangle$	6.3 (1.3)	10.0 (1.1)
$\langle Q_C^{EE-MCMM}\Phi_{Cl'}\rangle$	−3.4 (2.7)	−67.7 (9.4)
$\langle Q_C^{EE-MCMM}\Phi_{Cl}\rangle$	−149.6 (10.0)	−67.7 (9.4)
total	−148.4 (10.4)	−104.7 (8.6)

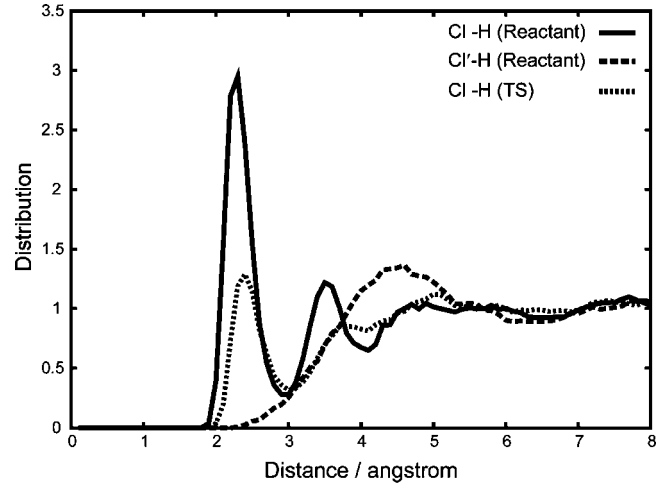

Figure 3. Radial distribution functions between the chloride in the solute and the hydrogen in solvent water: reactant Cl−H (solid line), reactant Cl′−H (dashed line), and TS Cl−H (dotted line).

The only difference between the present and previous studies is the number of Shepard points used in the EE−MCMM calculation. In the previous study, we used the electronic structure information at 12 Shepard points: three stationary points (the precursor ion−dipole complex, the saddle point, and the successor ion−dipole complex), eight nonstationary points along the minimum energy path (MEP), and one nonstationary point on the concave side of the reaction path. The ion−dipole complexes in the gas phase are located at $z = \pm 1.378$Å in the MPW1K calculation, and these 12 Shepard points are placed at $|z| \leq 1.378$ Å. To reproduce the PES at $|z| \geq 1.378$ Å, two additional Shepard points were added at $z = \pm 1.75$ Å; the remaining coordinates for these two additional points were optimized by direct gas-phase calculations. (Without these two additional Shepard points, total energy in the EE−MCMM/MM MD simulation was not conserved well at large $|z|$.) The locations of all 14 Shepard points and the direct MEP are shown in Figure 1. Note that six of the points are related to six others by symmetry, so one needs to calculate only eight Hessians as input to EE−MCMM. Note that, although the application is to a condensed-phase reaction, only electronic structure information for the gas-phase reaction is used.

For the QM/MM van der Waals interaction energy $V_{vdW}^{QM/MM}$, we used Lennard-Jones potentials. The Lennard-Jones param-

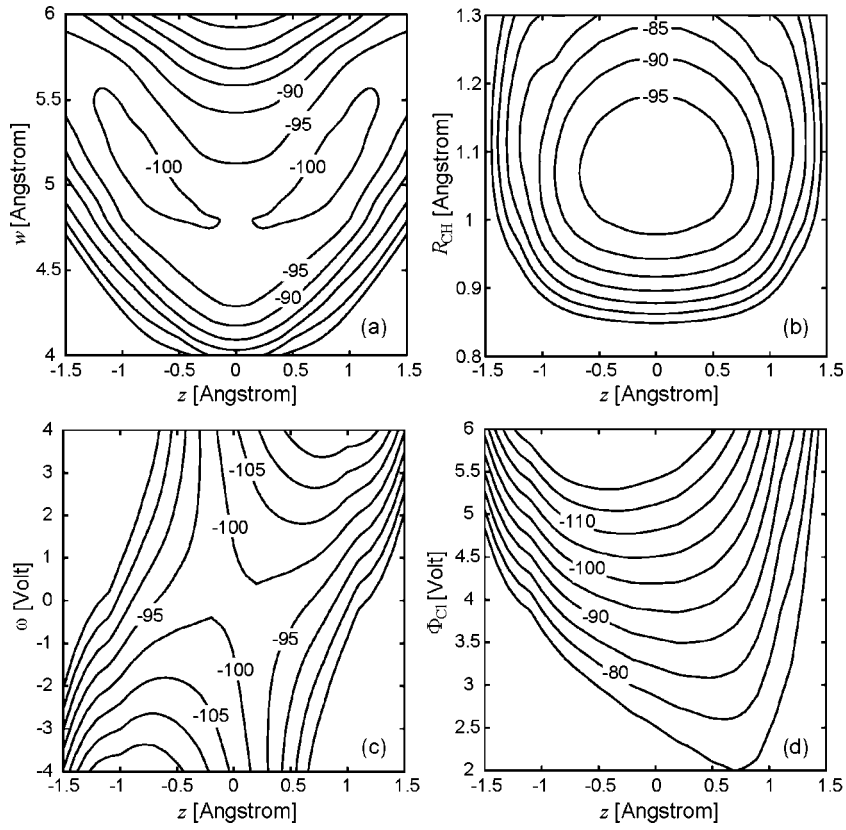

Figure 4. Equipotential contours of the EE−MCMM potential energy. The abscissa is the reaction coordinate z. The ordinate is (a) the sum of the length of the two C−Cl bonds, $w = R_{CCl} + R_{CCl'}$, (b) the length of the C−H bond, R_{CH}, (c) the difference between the electrostatic potential on the Cl atom and that on the Cl′ atom, $\omega = \Phi_{Cl'} - \Phi_{Cl}$, and (d) the electrostatic potential on the Cl atom, Φ_{Cl}. Contour labels are in kilocalories per mole. Contours are spaced (a) from −100 to −70, (b) from −95 to −65, (c) from −115 to −80, and (d) from −120 to −75 by 5 kcal/mol. The zero of energy is at infinitely separated reagents in the gas phase.

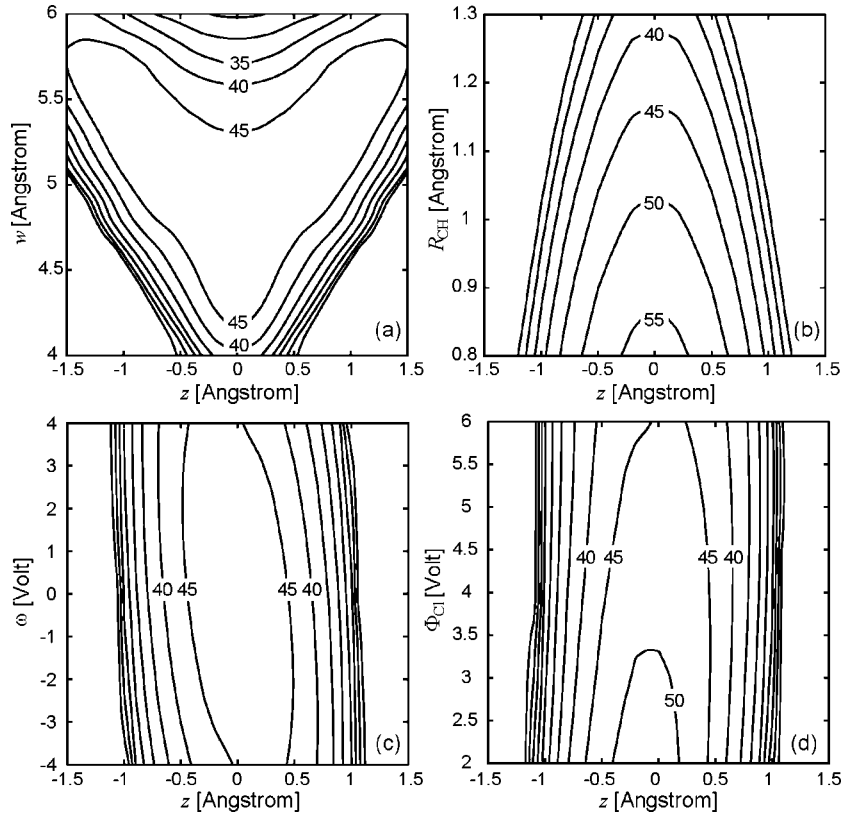

Figure 5. Equipotential contours of $U_{12}(\mathbf{q},\mathbf{\Phi})$. The axes are the same as in Figure 4. Contour labels are in kilocalories per mole. Contours are spaced (a) from 15 to 45, (b) from 25 to 55, (c) from 10 to 45, and (d) from 5 to 50 by 5 kcal/mol.

eters for the solute atoms were taken from the AMBER force field,[87] and the TIP3P model[88] was used for solvent−water molecules.

The EE−MCMM/MM MD simulation calculations were performed with periodic boundary conditions by the AMBER 9 package[89] combined with the MC-TINKER program. A cubic unit cell was used with a box length of 31.2 Å; this contains one solute ($Cl^- + CH_3Cl'$) and 1021 water molecules with a density of 1.0 g/cm^3 for water molecules. For the long-range electrostatic interaction, we used the tapering method implemented in the TINKER program,[90] where the electrostatic interaction smoothly becomes zero at 15 Å. A cutoff of 15 Å was also employed for the Lennard-Jones interactions. The equations of motion were integrated by the velocity Verlet method[91] with a time step of 0.5 fs at a temperature of 300 K. The SHAKE algorithm[92] was used to fix the intramolecular distances of the water solvent molecules.

To calculate the PMF along the reaction coordinate, we used the umbrella sampling method. We employed 21 umbrella sampling windows along the reaction coordinate z with harmonic restraining force constants 30−90 kcal mol^{-1} Å^{-2}. For each umbrella sampling window, we began with a 10 ps MD trajectory calculation for equilibration, followed by a 40 ps calculation for statistical sampling. The probability distributions for each window were pieced together with the weighted histogram analysis method[93–95] to compute the PMF.

4. Results and Discussion

The calculated aqueous PMF is presented in Figure 2. We also show the gas-phase potential energy profile along the reaction coordinate of the gas-phase reaction in Figure 2. The two curves are quite different because of the solute−solvent interaction. The free energy barrier between the reactant ($z = -2.0$ Å) and the transition state (TS; $z = 0.0$ Å) is found to be 25.3 kcal/mol, which agrees well with the experimental[96] activation free energy, 26.6 kcal/mol, and with previous[46] theoretical work.

In order to understand the differences between the QM/MM electrostatic interaction energy at the reactant and at the TS, we compared the contributions from the individual solute atoms according to eq 10. Note that the partial charges as well as the electrostatic potentials fluctuate in the EE−MCMM/MM MD simulation; therefore we averaged $Q_a^{\mathrm{EE-MCMM}}\Phi_a$ over the trajectories corresponding to a finite interval around a given value of z. (In particular, the trajectories with -0.05 Å $\le z \le +0.05$ Å were averaged to obtain the value for the TS, $z = 0.0$ Å, and the trajectories with $z = -2.0$ Å $\pm$ 0.05 Å were averaged for the reactant, $z = 2.0$ Å.) The results are shown in Table 1. The table shows that the chloride anion in the reactant interacts strongly with the solvent. In fact, the radial distribution functions between the chloride in the solute and the hydrogen atoms of water show much different character for the reactant and the TS (Figure 3). The sharp peak between the chloride anion and hydrogen at the reactant is a signature of the strong hydrogen bonding. There are no peaks in the first solvation shell between the chlorine atom of CH_3Cl and hydrogen. The standard deviations of the QM/MM electrostatic interaction energies are also shown in Table 1. The ratio of the standard deviation to the value of $\langle Q_{\mathrm{Cl}}^{\mathrm{EE-MCMM}}\Phi_{\mathrm{Cl}}\rangle$ at the TS is larger than that at the reactant. These fluctuations of the interaction energies are related to the fluctuations of the charges; the charge fluctuation at the reactant is smaller because the charge of the chloride anion is almost equal to -1 in the MD simulation, with a standard deviation of only 0.005, whereas the average value of the charge on either chlorine at the TS is -0.703, with a standard deviation of 0.034. This may be compared to the gas-phase charge on the chlorine at the gas-phase TS, which is -0.645.

Table 2. Average Values and Standard Deviations of Matrix Elements and EE−MCMM Energy at the TS in the EE−MCMM/MM MD Simulation.

	average	standard deviation
U_{11}, U_{22}	−47.7	11.7
U_{12}	49.0	2.1
$V^{\mathrm{EE-MCMM}}$	−97.2	8.6

We present equipotential contour plots of the EE−MCMM potential energy and $U_{12}(\mathbf{q},\mathbf{\Phi})$ in Figures 4 and 5. The abscissa is taken as the reaction coordinate z, and the ordinate is (a) the sum of the length of the two C−Cl bonds, $w = R_{\mathrm{CCl}} + R_{\mathrm{CCl'}}$, (b) the length of the C−H bond, R_{CH}, (c) the difference between the electrostatic potential on the Cl atom and that on the Cl′ atom, $\omega = \Phi_{\mathrm{Cl'}} - \Phi_{\mathrm{Cl}}$, and (d) the electrostatic potential on the Cl atom, Φ_{Cl}. The remaining coordinates are taken from the gas-phase TS geometry ($R_{\mathrm{CH}} = 1.065$ Å, $w = 4.594$ Å, and $\angle\mathrm{HCCl} = \angle\mathrm{HCCl'} = 90°$), and the remaining electrostatic potentials in the electrostatic potential distribution are taken from the average electrostatic potential during the EE−MCMM/MM MD simulation at the TS ($\Phi_{\mathrm{C}} = 3.444$ V, $\Phi_{\mathrm{H}} = 3.314$ V, $\Phi_{\mathrm{Cl}} = \Phi_{\mathrm{Cl'}} = 4.162$ V, and, in case c, $\Phi_{\mathrm{Cl}} + \Phi_{\mathrm{Cl'}} = 8.324$ V). The change of U_{12} is smaller than that of the EE−MCMM potential energy because the diagonal terms U_{11} and U_{22} can describe the main change of the EE−MCMM potential energy at the reactant and product. Although the effects of the electrostatic potential $\mathbf{\Phi}$ on U_{12} are smaller, U_{12} surely depends on $\mathbf{\Phi}$. Therefore, it is important to consider the dependence of U_{12} on the external electrostatic potential $\mathbf{\Phi}$. Table 2 shows average values and standard deviations of the matrix elements of $\mathbf{U}^{\mathrm{EE-MCMM}}$ and the EE−MCMM potential energy $V^{\mathrm{EE-MCMM}}$ at the TS in the EE−MCMM/MM MD simulation. The standard deviation of U_{12} is smaller than that of $V^{\mathrm{EE-MCMM}}$, which indicates that the change of U_{12} is smaller than that of $V^{\mathrm{EE-MCMM}}$ as in the case of Figures 4 and 5.

In previous work,[42] two different strategies, called QM/MM−MCMM and MCMM/MM, were proposed for combining MCMM with MM, and QM/MM−MCMM was applied to the reaction of complex molecules in the gas phase. The number, N^{MM}, of MM atoms in these examples was 4 and 24, respectively. The present EE−MCMM/MM approach is more similar to MCMM/MM; however, it eliminates the chief drawback of MCMM/MM, namely, that it corresponds to mechanical embedding, whereas EE−MCMM/MM corresponds to electrostatic embedding. This was an unfortunate disadvantage of MCMM/MM because it had the attractive feature of requiring one to handle only $3N^{\mathrm{QM}} \times 3N^{\mathrm{QM}}$ Hessians, whereas the Hessian size in QM/MM–MCMM is $3(N^{\mathrm{QM}} + N^{\mathrm{MM}}) \times 3(N^{\mathrm{QM}} + N^{\mathrm{MM}})$, which would be cumbersome (unless simplifying approximations were made) for simulating enzyme-catalyzed reactions for which N^{MM} is larger than N^{QM} by a factor of 10^2 or 10^3. The need for electrostatic embedding rather than

mechanical embedding has been emphasized elsewhere,[5,8,10,15,17,33,34,97] and the arguments need not be repeated here. EE−MCMM/MM includes electrostatic embedding, but it keeps the QM Hessian size manageable, at $4N^{QM} \times 4N^{QM}$. Note that the simulations reported here involve 1.05 ns of simulation time with a time step of 0.5 fs. Since the velocity Verlet algorithm requires one gradient per step, the total number of gradient calculations is 2.1×10^6. In a direct dynamics calculation, this would require 2.1×10^6 electronic structure gradients. However, the EE−MCMM input is only eight 24×24 Hessians. If the Hessians with respect to coordinates were evaluated by central differences of gradients and the Hessians with respect to electrostatic potentials were evaluated by central differences of charges, this would require only 2.7×10^3 gradient calculations and 2.1×10^3 charge calculations. The effort for QM calculations is thereby reduced by more than a factor 500. (Note that, because the first derivatives with respect to the electrostatic potentials are the partial charges, as shown in eq 4, the computational cost to calculate them is much lower than that to calculate the first derivatives with respect to the coordinates. Note also that if the symmetry of the solute molecule is considered, the number of gradient calculations is much lower.) If analytic Hessians[98] or partial Hessians[39] are employed, the savings are even greater, and if simulation times longer than 1.05 ns are considered, the electronic structure cost for direct dynamics is proportional to simulation time, whereas the electronic structure cost of EE−MCMM is fixed.

5. Conclusion

In the present study, we presented a combined EE−MCMM and MM method by replacing the electrostatically embedded QM energy in QM/MM with the EE−MCMM potential energy. We illustrated this method by applying it to carry out a molecular dynamics simulation of the reaction $Cl^- + CH_3Cl' \rightarrow ClCH_3 + Cl'^-$ in aqueous solution using hybrid DFT for the QM region. We used these EE−MCMM/MM MD simulations to compute the PMF. The free energy barrier is calculated to be 25.3 kcal/mol, which is in good agreement with the experimental estimates. We also compared the contribution from the individual solute atoms of the QM/MM electrostatic interaction energy.

On the basis of the present results, we conclude that the EE−MCMM/MM method is a very powerful tool for studying reactions in the condensed phase. It is noteworthy that it is straightforward (using, for example, link atom methods that have been extensively developed[2,3,6,8,10,17,20,29,97,99–101] in the context of previous QM/MM methods) to apply this method to a system that involves covalent bonds between the QM and MM regions, such as many reactions catalyzed by enzymes or heterogeneous catalysts.

Acknowledgment. This work is supported by the National Science Foundation by grant no. CHE07-04974.

References

(1) Warshel, A.; Levitt, M. *J. Mol. Biol.* **1976**, *103*, 227.

(2) Singh, U. C.; Kollman, P. A. *J. Comput. Chem.* **1986**, *7*, 718.

(3) Field, M. J.; Bash, P. A.; Karplus, M. *J. Comput. Chem.* **1990**, *11*, 700.

(4) Gao, J. *Acc. Chem. Res.* **1996**, *29*, 298.

(5) Bakowies, D.; Thiel, W. *J. Phys. Chem.* **1996**, *100*, 10580.

(6) Eurenius, K. P.; Chatfield, D. C.; Brooks, B. R.; Hodoscek, M. *Int. J. Quantum Chem.* **1996**, *60*, 1189.

(7) Truong, T. N.; Truong, T.-T.; Stefanovich, E. V. *J. Chem. Phys.* **1997**, *107*, 1881.

(8) Antés, I.; Thiel, W. In *Combined Quantum Mechanical and Molecular Mechanical Methods*; Gao, J., Thompson, M. A., Eds.; American Chemical Society: Washington, DC, 1998; ACS Symposium Series 712, p 50.

(9) Tongraar, A.; Liedl, K. R.; Rode, B. M. *J. Phys. Chem. A* **1998**, *102*, 10340.

(10) Burton, N. A.; Harrison, M. J.; Hart, J.; Hillier, I. H.; Sheppard, D. W. *Faraday Discuss.* **1998**, *110*, 463.

(11) Zhang, Y.; Lee, T.-S.; Yang, W. *J. Chem. Phys.* **1999**, *110*, 46.

(12) Philipp, D. M.; Friesner, R. A. *J. Comput. Chem.* **1999**, *20*, 1468.

(13) Eichinger, M.; Tavan, P.; Hutter, J.; Parrinello, M. *J. Chem. Phys.* **1999**, *110*, 10452.

(14) Woo, T. K.; Blöchl, P. E.; Ziegler, T. *J. Phys. Chem. A* **2000**, *104*, 121.

(15) Reuter, N.; Dejaegere, A.; Maigret, B.; Karplus, M. *J. Phys. Chem. A* **2000**, *104*, 1720.

(16) Gogonea, V.; Westerhoff, L. M.; Merz, K. M., Jr *J. Chem. Phys.* **2000**, *113*, 5604.

(17) Sherwood, P. In *Modern Methods and Algorithms of Quantum Chemistry*; Grotendorst, J., Ed.; John von Neumann Institute for Computing: Jülich, Germany, 2000; Vol. NIC Series 3, p 285.

(18) Chalmet, S.; Rinaldi, D.; Ruiz-Lopez, M. F. *Int. J. Quantum Chem.* **2001**, *84*, 559.

(19) Martí, S.; Andrés, J.; Moliner, V.; Silla, E.; Tuñón, I.; Bertrán, J. *Theor. Chem. Acc.* **2001**, *105*, 207.

(20) Gao, J.; Truhlar, D. G. *Annu. Rev. Phys. Chem.* **2002**, *53*, 467.

(21) Laio, A.; VandeVondele, J.; Rothlisberger, U. *J. Chem. Phys.* **2002**, *116*, 6941.

(22) Amara, P.; Field, M. J. *Theor. Chem. Acc.* **2003**, *109*, 43.

(23) Vreven, T.; Morokuma, K. *Theor. Chem. Acc.* **2003**, *109*, 125.

(24) Kerdcharoen, T.; Birkenheuer, U.; Krüger, S.; Woiterski, A.; Rösch, N. *Theor. Chem. Acc.* **2003**, *109*, 285.

(25) Nemukhin, A. V.; Grigorenko, B. L.; Topol, I. A.; Burt, S. K. *J. Comput. Chem.* **2003**, *24*, 1410.

(26) Garcia-Viloca, M.; Truhlar, D. G.; Gao, J. *J. Mol. Biol.* **2003**, *327*, 549.

(27) Toniolo, A.; Ciminelli, C.; Granucci, G.; Laino, T.; Persico, M. *Theor. Chem. Acc.* **2004**, *111*, 270.

(28) Bathelt, C. M.; Zurek, J.; Mulholland, A. J.; Harvey, J. N. *J. Am. Chem. Soc.* **2005**, *127*, 12900.

(29) Pu, J.; Gao, J.; Truhlar, D. G. *ChemPhysChem* **2005**, *6*, 1853.

(30) Sundararajan, M.; Hillier, I. H.; Burton, N. A. *J. Phys. Chem. A* **2006**, *110*, 785.

(31) Riccardi, D.; Schaefer, P.; Yang, Y.; Yu, H.; Ghosh, N.; Prat-Resina, X.; König, P.; Li, G.; Xu, D.; Guo, H.; Elstner, M.; Cui, Q. *J. Phys. Chem. B* **2006**, *110*, 6458.

(32) To, J.; Sherwood, P.; Sokol, A. A.; Bush, I. J.; Catlow, C. R. A.; van Dam, H. J. J.; French, S. A.; Guest, M. F. *J. Mater. Chem.* **2006**, *16*, 1919.

(33) Lin, H.; Truhlar, D. G. *Theor. Chem. Acc.* **2007**, *117*, 185.

(34) Senn, H. M.; Thiel, W. *Curr. Opinion Chem. Biol.* **2007**, *11*, 182.

(35) Woodcock, H. L., III; Hodošček, M.; Gilbert, A. T. B.; Gill, P. M. W.; Schaefer, H. F., III; Brooks, B. R. *J. Comput. Chem.* **2007**, *28*, 1485.

(36) Higashi, M.; Truhlar, D. G. *J. Chem. Theory Comput.* **2008**, *4*, 790.

(37) Kim, Y.; Corchado, J. C.; Villa, J.; Xing, J.; Truhlar, D. G. *J. Chem. Phys.* **2000**, *112*, 2718.

(38) Albu, T. V.; Corchado, J. C.; Truhlar, D. G. *J. Phys. Chem. A* **2001**, *105*, 8465.

(39) Lin, H.; Pu, J.; Albu, T. V.; Truhlar, D. G. *J. Phys. Chem. A* **2004**, *108*, 4112.

(40) Kim, K. H.; Kim, Y. *J. Chem. Phys.* **2004**, *120*, 623.

(41) Kim, Y.; Kim, Y. *J. Phys. Chem. A* **2006**, *110*, 600.

(42) Lin, H.; Zhao, Y.; Tishchenko, O.; Truhlar, D. G. *J. Chem. Theory Comput.* **2006**, *2*, 1237.

(43) Tishchenko, O.; Truhlar, D. G. *J. Phys. Chem. A* **2006**, *110*, 13530.

(44) Tishchenko, O.; Truhlar, D. G. *J. Chem. Theory Comput.* **2007**, *3*, 938.

(45) Chandrasekhar, J.; Smith, S. F.; Jorgensen, W. L. *J. Am. Chem. Soc.* **1984**, *106*, 3049.

(46) Chandrasekhar, J.; Smith, S. F.; Jorgensen, W. L. *J. Am. Chem. Soc.* **1985**, *107*, 154.

(47) Bash, P. A.; Field, M. J.; Karplus, M. *J. Am. Chem. Soc.* **1987**, *109*, 8092.

(48) Kozaki, T.; Morihashi, K.; Kikuchi, O. *J. Am. Chem. Soc.* **1989**, *111*, 1547.

(49) Huston, S. E.; Rossky, P. J.; Zichi, D. A. *J. Am. Chem. Soc.* **1989**, *111*, 5680.

(50) Tucker, S. C.; Truhlar, D. G. *J. Am. Chem. Soc.* **1990**, *112*, 3347.

(51) Zhao, X. G.; Tucker, S. C.; Truhlar, D. G. *J. Am. Chem. Soc.* **1991**, *113*, 826.

(52) Basilevsky, M. V.; Chudinov, G. E.; Napolov, D. V. *J. Phys. Chem.* **1993**, *97*, 3270.

(53) Mathis, J. R.; Bianco, R.; Hynes, J. T. *J. Mol. Liq.* **1994**, *61*, 81.

(54) Truong, T. N.; Stefanovich, E. V. *J. Phys. Chem.* **1995**, *99*, 14700.

(55) Pomelli, C. S.; Tomasi, J. *J. Phys. Chem. A* **1997**, *101*, 3561.

(56) Cossi, M.; Adamo, C.; Barone, V. *Chem. Phys. Lett.* **1998**, *297*, 1.

(57) Mo, Y.; Gao, J. *J. Comput. Chem.* **2000**, *21*, 1458.

(58) Safi, B.; Choho, K.; Geerlings, P. *J. Phys. Chem. A* **2001**, *105*, 591.

(59) Ohmiya, K.; Kato, S. *Chem. Phys. Lett.* **2001**, *348*, 75.

(60) Gao, J.; Garcia-Viloca, M.; Poulsen, T. D.; Mo, Y. *Adv. Phys. Org. Chem.* **2003**, *38*, 161.

(61) Mo, S. J.; Vreven, T.; Mennucci, B.; Morokuma, K.; Tomasi, J. *Theor. Chem. Acc.* **2004**, *111*, 154.

(62) Vayner, G.; Houk, K. N.; Jorgensen, W. L.; Brauman, J. I. *J. Am. Chem. Soc.* **2004**, *126*, 9054.

(63) Sato, H.; Sakaki, S. *J. Phys. Chem. A* **2004**, *108*, 1629.

(64) Freedman, H.; Truong, T. N. *J. Phys. Chem. B* **2005**, *109*, 4726.

(65) Song, L.; Wu, W.; Hiberty, P. C.; Shaik, S. *Chem.—Eur. J.* **2006**, *12*, 7458.

(66) Casanova, D.; Gusarov, S.; Kovalenko, A.; Ziegler, T. *J. Chem. Theory Comput.* **2007**, *3*, 458.

(67) Su, P.; Wu, W.; Kelly, C. P.; Cramer, C. J.; Truhlar, D. G. *J. Phys. Chem. A*, In press.

(68) Hu, H.; Lu, Z.; Parks, J. M.; Burger, S. K.; Yang, W. *J. Chem. Phys.* **2008**, *128*, 034105.

(69) Ten-no, S.; Hirata, F.; Kato, S. *Chem. Phys. Lett.* **1993**, *214*, 391.

(70) Ten-no, S.; Hirata, F.; Kato, S. *J. Chem. Phys.* **1994**, *100*, 7443.

(71) Sato, H.; Hirata, F.; Kato, S. *J. Chem. Phys.* **1996**, *105*, 1546.

(72) Bayly, C. I.; Cieplak, P.; Cornell, W. D.; Kollman, P. A. *J. Phys. Chem.* **1993**, *97*, 10269.

(73) Morita, A.; Kato, S. *J. Am. Chem. Soc.* **1997**, *119*, 4021.

(74) Morita, A.; Kato, S. *J. Chem. Phys.* **1998**, *108*, 6809.

(75) Hayashi, S.; Ohmine, I. *J. Phys. Chem. B* **2000**, *104*, 10678.

(76) Wilson, E. B., Jr.; Decius, J. C.; Cross, P. C. *Molecular Vibrations*; Dover: New York, 1955.

(77) Tishchenko, O.; Higashi, M.; Albu, T. V.; Corchado, J. C.; Kim, Y.; Villà, J.; Xing, J.; Lin, H.; Truhlar, D. G. *MC-TINKER*, version 2008; University of Minnesota: Minneapolis, MN, 2008. The correct analytical gradient of the MCMM energy with respect to the coordinates is given in the manual of this program [Tishchenko and Truhlar, Apendix: *MCMM Equations*, July 11, 2007, http://comp.chem.umn.edu/mc-tinker/MCMM-APPENDIX.pdf (accessed April 19, 2008)].

(78) Ischtwan, J.; Collins, M. A. *J. Chem. Phys.* **1994**, *100*, 8080.

(79) Nguyen, K. A.; Rossi, I.; Truhlar, D. G. *J. Chem. Phys.* **1995**, *103*, 5522.

(80) Lynch, B. J.; Fast, P. L.; Harris, M.; Truhlar, D. G. *J. Phys. Chem. A* **2000**, *104*, 4811.

(81) Kelly, C. P.; Cramer, C. J.; Truhlar, D. G. *J. Chem. Theory Comput.* **2005**, *1*, 1133.

(82) Higashi, M.; Chamberlin, A. C.; Pu, J.; Kelly, C. P.; Thompson, J. D.; Xidos, J. D.; Li, J.; Zhu, T.; Hawkins, G. D.; Chuang, Y.-Y.; Fast, P. L.; Lynch, B. J.; Liotard, D. A.; Rinaldi, D.; Gao, J.; Cramer, C. J.; Truhlar, D. G. *GAMESSPLUS*, version 2008; University of Minnesota: Minneapolis, MN, 2008.

(83) Schmidt, M. W.; Baldridge, K. K.; Boatz, J. A.; Elbert, S. T.; Gordon, M. S.; Jensen, J. H.; Koseki, S.; Matsunaga, N.; Nguyen, K. A.; Su, S. J.; Windus, T. L.; Dupuis, M.; Montgomery, J. A. *J. Comput. Chem.* **1993**, *14*, 1347.

(84) Allinger, N. L.; Yuh, Y. H.; Lii, J. H. *J. Am. Chem. Soc.* **1989**, *111*, 8551.

(85) Lii, J. H.; Allinger, N. L. *J. Am. Chem. Soc.* **1989**, *111*, 8566.

(86) Lii, J. H.; Allinger, N. L. *J. Am. Chem. Soc.* **1989**, *111*, 8576.

(87) Cornell, W. D.; Cieplak, P.; Bayly, C. I.; Gould, I. R.; Merz, K. M., Jr.; Ferguson, D. M.; Spellmeyer, D. G.; Fox, T.; Caldwell, J. W.; Kollman, P. A. *J. Am. Chem. Soc.* **1995**, *117*, 5179.

(88) Jorgensen, W. L.; Chandrasekhar, J.; Madura, J. D.; Impey, R. W.; Klein, M. L. *J. Chem. Phys.* **1983**, *79*, 926.

(89) Case, D. A.; Darden, T. A.; Cheatham, I. T. E.; Simmerling, C. L.; Wang, J.; Duke, R. E.; Luo, R.; Merz, K. M.; Pearlman, D. A.; Crowley, M.; Walker, R. C.; Zhang, W.; Wang, B.; Hayik, S.; Roitberg, A.; Seabra, G.; Wong, K. F.; Paesani, F.; Wu, X.; Brozell, S.; Tsui, V.; Gohlke, H.; Yang, L.; Tan, C.; Mongan, J.; Hornak, V.; Cui, G.; Beroza, P.; Mathews, D. H.; Schafmeister, C.; Ross, W. S.; Kollman, P. A. *AMBER 9*; University of California: San Francisco, CA, 2006.

(90) Ponder, J. W. *TINKER*, version 3.5; Washington University: St. Louis, MO, 1997.

(91) Swope, W. C.; Andersen, H. C.; Berens, P. H.; Wilson, K. R. *J. Chem. Phys.* **1982**, *76*, 637.

(92) Miyamoto, S.; Kollman, P. A. *J. Comput. Chem.* **1992**, *13*, 952.

(93) Kumar, S.; Bouzida, D.; Swendsen, R. H.; Kollman, P. A.; Rosenberg, J. M. *J. Comput. Chem.* **1992**, *13*, 1011.

(94) Kumar, S.; Rosenberg, J. M.; Bouzida, D.; Swendsen, R. H.; Kollman, P. A. *J. Comput. Chem.* **1995**, *16*, 1339.

(95) Roux, B. *Comput. Phys. Commun.* **1995**, *91*, 275.

(96) McLennan, D. J. *Aust. J. Chem.* **1978**, *31*, 1897.

(97) Zhang, Y.; Lin, H.; Truhlar, D. G. *J. Chem. Theory Comput.* **2007**, *3*, 1378.

(98) Burant, J. C.; Strain, M. C.; Scuseria, G. E.; Frisch, M. J. *Chem. Phys. Lett.* **1996**, *258*, 45.

(99) König, P. H.; Hoffmann, M.; Frauenheim, Th.; Cui, Q. *J. Phys. Chem. B* **2005**, *109*, 9082.

(100) Pu, J.; Gao, J.; Truhlar, D. G. *J. Phys. Chem. A* **2004**, *108*, 632.

(101) Lin, H.; Truhlar, D. G. *J. Phys. Chem. A* **2005**, *109*, 3991.

CT8000816